Experimenting with learning-based image orientation approaches for photogrammetric mapping of *Posidonia oceanica* meadows

Fabio Menna [1], Alessio Calantropio [2], Arianna Pansini[1], Giulia Ceccherelli[1], Erica Nocerino [3]

[1] Department of Chemical, Physical, Mathematical and Natural Sciences, University of Sassari, Sassari, Italy – (fmenna; apansini; cecche) @uniss.it
[2] Department of Science and Technology, University of Napoli Parthenope, Napoli, Italy – alessio@calantropio.it
[3] Department of Humanities and Social Sciences, University of Sassari, Sassari, Italy - enocerino@uniss.it

Keywords: *Posidonia Oceanica*, Deep Learning, Underwater Photogrammetry, Feature Extraction, Feature Matching, Structure-From-Motion, Artificial Intelligence.

Abstract

Posidonia oceanica (L.) Delile (PO) is an endemic seagrass of the Mediterranean Sea, where it grows in the form of dense meadows extending from the surface up to 40 m depth. PO plays a key role in the underwater realm, providing numerous ecosystem services, but it is nowadays endangered by climate change and anthropogenic pressure. Its evolution is therefore monitored following protocols recommended by national environmental agencies. In the literature, optical imaging technologies have been tested for mapping and monitoring PO, although no studies have systematically investigated how the non-static, threadlike, characteristics of PO negatively impact the underwater photogrammetry workflow. To optimize and complement current monitoring practices, the POSEIDON project is currently investigating a multi-resolution, multi-technique geomatic approach. Within POSEIDON, this study focuses on the use of beyond ultra-high resolution (BUHR) underwater photogrammetry and highlights the critical aspects involved in surveying a complex, moving environment such as extended continuous PO meadows. A comparative analysis of traditional algorithms and AI-driven approaches for image orientation is presented on datasets that differ by acquisition protocols, depth, season, platform type, and imaging system. Although some learning-based methods seemed to perform better than hand-crafted ones, we could not identify a winning method. Moreover we verified that, in such a complex scenario, it is crucial to adjust processing thresholds at the different stages of SfM (from matching to bundle adjustment) and take manual intervention measures to improve image orientation.

1. Introduction

The endemic *Posidonia oceanica* (L.) Delile (PO) is the most abundant seagrass in the Mediterranean Sea where it forms extensive meadows from the surface down to 40 m depth (Vassallo et al., 2013). PO provides numerous ecosystem services that help maintain marine coastal environments and mitigate climate change effects, such as oxygen production, carbon sequestration, coastal erosion prevention, nursery and shelter for different species, water quality improvement, to cite a few. However, at the same time, PO is threatened by climate change and anthropogenic pressure; as such, it is recognised as an endangered protected species under different European and national regulations. Because of its key role in the Mediterranean Sea, PO is monitored according to protocols provided by national environmental agencies. Moreover, numerous scientific initiatives have been activated to assist the recovery of PO through restoration programs (Pansini et al., 2025). To help answer the growing demand for effective and reliable monitoring methods, in recent years, the scientific community has undertaken great efforts in developing innovative methods for mapping PO using optical imaging methodologies from space, surface, and underwater (Appolloni et al., 2020; Baiocchi et al., 2024; Bonin-Font et al., 2016; Cozza et al., 2019; Dattola et al., 2018; Mandlburger, 2022).

1.1 The POSEIDON project

Within this panorama, the POSEIDON (multitemPOral SEagrass mapping and monitoring of posIDONia meadows and banquettes for blue carbon conservation) project, funded by the Italian National Recovery and Resilience Plan (PNRR), aims to study, develop, and test new geomatic methodologies for mapping and monitoring PO meadows and banquettes in the Mediterranean area (Ceccherelli et al., 2024). Among the different developed techniques, the project demonstrates and validates the use of underwater photogrammetry for 3D documentation and mapping of PO, leveraging the higher resolution provided by optical imaging compared to sonar and other remote sensing techniques.

Current 3D reconstruction techniques, based on photogrammetric algorithms, present additional challenges when applied to underwater scenarios, particularly on seagrasses like PO. We present here some experiences carried out within the POSEIDON project in surveying PO meadows by underwater photogrammetry in different conditions and depths, from the upper limit in shallow water (2-3 m) down to 15 m, a reference depth used by the Italian agency for environmental research and protection (ISPRA).

1.2 Related works on monitoring *Posidonia oceanica* with underwater photogrammetry

Several studies presented the application of underwater photogrammetry for high-resolution mapping and monitoring of PO, providing a methodological approach to surveying the boundary limits of PO meadow (Abadie et al., 2018; Marre et al., 2020; Russo et al., 2023) and carrying out morphological measurements (Rende et al., 2022; 2020; 2015), such as leaf height. Many of these studies use image or point cloud segmentation to automatically distinguish between PO and other seabed substrate elements, mostly dead matte or dead leaves.

Most studies classify PO using object-based image analysis (Rende et al., 2022; Ventura et al., 2022), while Marre et al. (2020) use heuristics, such as the greater spatial uncertainty

associated with tie points measured on PO leaves, mainly caused by leaf motion.

1.3 A strong assumption: a still substrate

Some of the studies reported above focused on monitoring the evolution of boundaries of PO meadows (progression vs regression), especially in restoration fields, where PO patches are transplanted after being collected from nearby areas. These premises depict an underwater environment where the PO is not present as a continuous meadow but rather as a field of discontinuous patches scattered at the seabed and interleaved by a more stable substrate, such as dead matte, sand, or rocks. Therefore, the strongest assumption made is that the surveyed area is not fully covered by PO and that at least a portion of the field of view of each image used for the photogrammetric process observes the stable substrate of the PO restoration field.

These conditions are likely met in restoration fields, although larger and continuous patches of PO leaves can be present, existing before the restoration field was set. In such cases, parts of the images composing the photogrammetric block could still observe areas entirely covered by PO leaves, with image orientation relying on tie points observed on a non-rigid, potentially moving substrate.

We could not find studies about the use of photogrammetry in an area with an extended, continuous PO meadow.

1.4 Open challenges in *Posidonia oceanica* photogrammetric surveys

One of the most significant challenges in surveying PO is the non-static, threadlike, characteristics of the leaves that make it very difficult for photogrammetric algorithms to correctly orient the images, and subsequently generate products, such as dense point clouds and orthophoto mosaics.

When elongated leaves overlap, apparent corner-like intersections and self-occlusions are created that vary with the viewpoint. Figure 1 shows a close-up view of an image pair taken over a PO meadow. Between the left and right images, the leaves are still, given the synchronous acquisition. The image shows that PO leaves create apparent sliding intersections and self-occlusions that vary with the viewpoint whenever leaves are not lying on the same plane. Automatic feature description and matching approaches are thus strongly influenced, making image orientation using points extracted on PO very difficult.

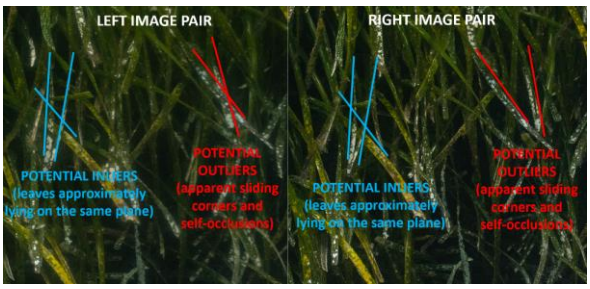

Figure 1. Challenges in feature detection, description and matching of PO meadows: apparent corner-like intersections and self-occlusions are created and vary with the viewpoint.

Moreover, the movement of leaves, especially the longer ones, invalidates the rigid body assumption made in photogrammetry concerning the observed scene.

Additionally, depending on several environmental factors as the depth, weather, season, and the imaging system used (Figure 2), the leaves may appear featureless, creating repetitive patterns difficult to match due to not enough discriminative descriptors. In Figure 2, the left image is a close-up view of a PO meadow acquired with a Micro Four Thirds underwater camera system during a sunny summer day. On the right, an image frame is extracted from a 4K resolution video recorded using a GoPro 12 at 15m depth during a cloudy winter day. The left image shows greater information due to the presence of epiphytes and leaf incrustations, the richer light available in shallow water, and the better signal-to-noise imaging technology.

To the best of our knowledge, there are no studies reporting on the use of underwater photogrammetry over PO focusing on these challenges and potential related errors.

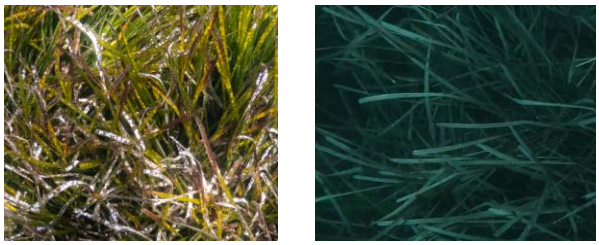

Figure 2. Different visual appearance of PO leaves depending on several environmental factors and technology used.

1.5 Our approach using learning-based image orientation on *Posidonia Oceanica*

Recent developments in artificial intelligence and its use in image orientation examined matching performances of learning-based versus hand-crafted methods (Chen et al., 2020; Remondino et al., 2021; Zhong et al., 2024). For this task, specific tools were developed, such as Deep-Image-Matching (Morelli et al., 2024), an open-source toolbox designed to test different hand-crafted and learning-based image orientation approaches

In this contribution, we use Deep-Image-Matching (DIM), comparing traditional algorithms, with AI-driven approaches in image orientation of photogrammetric surveys over PO, focusing on the most challenging scenario of full meadows or cases where a few images along the strip are observing only PO. The aim is to provide a preliminary analysis on the accuracy and reliability of novel as well as more traditional image orientation methods for photogrammetric mapping of large areas covered by PO.

2. Material and methods

2.1 Rationale of the experiments and underwater datasets

We conducted different experiments to understand how the morphological characteristics of PO, environmental conditions, imaging technology, and survey execution affect image orientation approaches, both hand-crafted and learning-based, over substrates covered by PO.

The research utilises beyond ultra-high resolution (BUHR) image datasets with ground sample distance (GSD) better than 2 mm acquired within the POSEIDON project along the Northwest coast of Sardinia Island, Italy, in different locations, seasons, depths, and weather conditions, spanning various real-world scenarios of the Mediterranean Sea.

Figure 3. Location of the experimental sites where the datasets detailed in Table 1 were collected (left and middle - source Google Earth); USV platform and SCUBA diver at the site location (right column).

Dataset	Survey Type/ size	PO characteristics/ Depth	Season	Platform type/ speed	Camera system/ Image acquisition mode/ UW housing type	# images / GSD
A	Straight transect 45deg forward looking (50x) m^2	Discontinuous meadow/ 0.7-2 m (upper limit)	Winter	USV/ 1.0 m/s	GoPro 10 action camera/ 2Hz Still frames	100/ 0.6 mm
B1	Full block/ (22x7) m^2	Continuous meadow/ 15 m	Autumn	Diver operated/ 0.25 m/s	2 x GoPro 12 action cameras in stereo configuration/ 2 Hz 4K video frames/ flat port	1178/ 1.0 mm
B2	Full block (22x7) m^2	Continuous meadow/ 15 m	Winter	Diver operated/ 0.25 m/s	Single Nikon D850 46MP DSLR/ 1 Hz timelapse images/ centered dome port	910/ 0.35 mm
C	Square loop/ (50x3) m^2	Continuous meadow/ 3-4 m (upper limit)	Summer	Diver operated/ 0.25 m/s	Single Nikon D850 46MP DSLR/ 1 Hz timelapse images/ centered dome port	304/ 0.35 mm

Table 1. Characteristics of the dataset used in the presented study

Single and synchronised stereo-camera systems, ranging from GoPro action cameras to full-frame DSLRs, were utilized. The selected datasets feature many of the specific challenges described in section 1.4 and were collected in the Bay of Porto Conte, near Alghero, Italy (Figure 3). They comprise different image acquisition protocols, from simple transects to larger rectangular plots as described hereafter and summarised in Table 1:

Dataset A is a 50 m long transect obtained by extracting a single strip from a larger survey using an uncrewed surface vehicle (USV), the BlueBoat catamaran from Blue Robotics[1]. The BlueBoat was used as an autonomous platform carrying a GoPro 10 underwater inclined at about 45 degrees off-nadir. The images were acquired at 2Hz in timelapse mode. The first half of the transect featured only dead matte at a depth of about 2m, an easier substrate to match between the images; in the second half of the transect, the depth reduced significantly up to the minimum depth of 0.7m, thus lowering the overlap between subsequent images, and the seabed became fully covered by the PO meadow. The image scale variations, the wide baseline and the light caustics, represent the greatest challenges of this dataset.

Dataset B1 and B2 are full photogrammetric blocks covering about (7x22) m^2 at 15 m depth over a continuous meadow (density of 231 shoots/ m^2). Dataset B1 was taken at the end of autumn, when the senescent leaves are still attached to the shoots. The weather conditions were favourable: the sea was calm, and slight motion of the PO leaves was observed during the survey. Light conditions were variable due to an alternating cloudy and sunny day. 4K videos from two GoPro 12 action cameras in stereo configuration were recorded. GoPro HyperSmooth video stabilisation was deactivated to avoid introducing unmodelled systematic effects into the photogrammetric workflow (Nocerino et al., 2022). Dataset B2 was acquired in late winter, when the leaves attached to the shoots were less dense, and the matte patches underneath were visible in some areas. A single full-frame DSLR camera, characterised by a wider dynamic range, was used. In this dataset, the motion of the PO leaves could be observed due to the swell. These two datasets provide a baseline comparison for understanding how the seasonal cycle of PO meadow with its different morphological characteristics (i.e., longer leaves, presence of senescent leaves, denser foliage coverage). affect image matching.

[1] bluerobotics.com

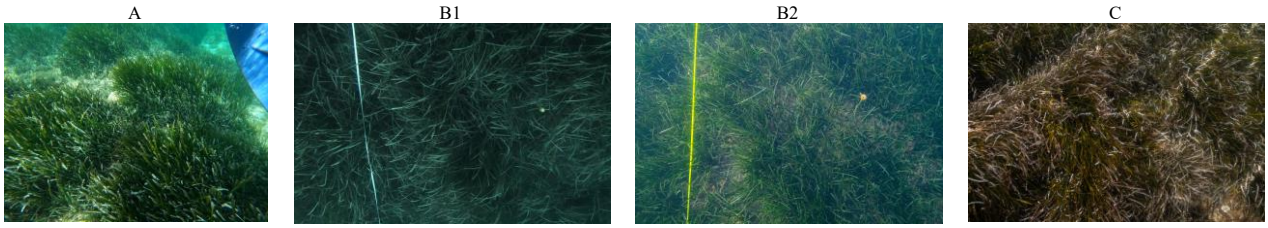

Figure 4. Illustrative images from the different datasets. B1 and B2 show the same area in two different seasons: in winter (B2), the leaves are sparser and shorter, thus allowing the matte to be spot; in contrast, in autumn (B1), the leaves are longer and denser, and the matte is not visible.

Dataset C is a square loop captured during summer over a shallow site (4m depth) at the upper limit of the PO meadow. The main challenges are the long PO leaves and the presence of light caustics from the water surface.

The loop was captured keeping the field of view of the camera over the continuous part of the meadow. The substrate was a mix of matte and rocks, with a few rocks occasionally visible in some images. The sunny summer day and the shallow site make the light rich in colours and contrast. Epiphytes and other finely detailed leaf characteristics like the presence of bytes and damaged leaf tips are visible.

2.2 Underwater camera systems, synch, and calibration

Considering the challenges described in section 1.4, we did not plan to process the image datasets, letting the bundle adjustment solve for camera calibration parameters (self-calibration).
Indeed, several factors such as:

1) the high probability of outliers among the matched tie-points;
2) the difficulty to match natural points over PO between images with wide baselines, such as those belonging to different strips;
3) the weak imaging network (aerial-like nadiral acquisition);

made such a scenario unsuitable for self-calibration. In these circumstances, outliers would very likely be absorbed by the exterior orientation and camera calibration parameters.

Therefore, at the bottom of each underwater site, we set a temporary calibration field consisting of about 10 weighted rigid aluminium plates with four coded targets each for a total of 40 targets placed on the seabed and spread over an area approximately covering the field of view of the camera at the planned acquisition distance of the survey. Additionally, two scale bars, resolution, and colour checker targets were included for colour correction and image quality analysis (Figure 5 - right). The calibration plates and the scale bars were previously measured in laboratory with an estimated uncertainty of distances between targets better than 0.1mm.

The calibration dataset consisted, on average, of about 100 photographs taken all around the temporary calibration field, ensuring different attitudes, elevation, and roll diversity as required in regular camera calibration procedures in photogrammetry.

For the Nikon D850, for each dataset, we prefocused the camera at the distance planned over the PO field directly underwater through the dome port and kept the focusing unchanged for the entire dive.

We did not explicitly model the refractive effects of dome and flat ports. The dome port was centred through the procedure presented in Menna et al. (2016) while the distance between the flat port of the GoPro housing and the entrance pupil of the GoPro cameras was considered negligible for the purpose of this study (Menna et al., 2018).

The video synchronization for the dataset B1 was performed in post processing by aligning the video stream timelines using as synch event the activation of an underwater LED flashlight visible in the two cameras. The synch event was recorded at the beginning and at the end of the survey. This procedure allows a synchronisation error up to the duration of one frame, which was $1/60^{th}$ of a second.

2.3 Ground truth measurements

To quantitatively assess the performances of the investigated algorithms, we collected, whenever possible, ground truth measurements underwater using stable reference points materialized through 1m long poles inserted in the PO substrate for about half a meter. Length measurements (estimated accuracy 1 cm) and height differences (estimated accuracy 1 cm) between the top of the poles, made visible with a white cap, were collected using a tape meter and a custom-developed pressure sensor (Menna et al., 2024), respectively. When ground truth could not be measured, we acquired the images using either round trip transects (along a straight line) or loops (squares or rectangles) to check the ability to match revisited areas and use the loop closure as measure of the accumulated drift error. Additionally, two 1 m long scale bars were placed at the site location for scaling.

2.4 Photogrammetric processing workflow

We experimented with hand crafted and learning-based image orientation over PO using Agisoft Metashape (v2.2.0) commercial software, COLMAP (v3.11.1) and DIM (v1.0.0) open-source software applications. We used Metashape for estimating the camera calibration parameters using the calibration datasets (section 2.2) and then undistorting the survey images. This strategy was necessary to import COLMAP and DIM results in Metashape through the bundler format, which uses a simplified distortion model for camera calibration.

Figure 5. Images for calibration datasets on PO matte (left), PO meadow (centre). A detail of a resolution target (right)

Metashape and COLMAP were then used in a standard Structure-from-Motion image orientation workflow with a fixed pinhole camera calibration model and default processing parameters using brute-force matching for all the datasets. These tests provided a baseline for understanding the current limitations of hand-crafted SIFT-like feature extraction and matching approaches.

To test learning-based feature extraction and matching we used DIM with default parameters. Finally, all the image observations from DIM and COLMAP were imported in Metashape for carrying out all the manual measurements, such as collimating the scale bars targets and check points (CPs) (when needed for results assessment).

For the stereo camera configuration dataset B1we did not enforce any baseline constraint at the image orientation stage in COLMAP and DIM but applied the baseline constraint in a final bundle adjustment in Metashape. This was also the method used for scaling the survey B1. For B2 we used all the length measured for scaling along with the height measurements from the pressure sensor. We then analysed for B1and B2 the residuals on both the scale bars and CPs heights.

Whenever some images failed to orient in Metashape, we used the suggested manual procedure to unorient and then orient again (align) the manually selected images. This procedure worked only for dataset B1, where all the images could be oriented. In all the other cases the dataset could not be completely oriented in Metashape.

While with Metashape we had limited choice of advanced Structure-from-Motion processing parameters, with COLMAP and DIM if a dataset could not be oriented completely with default parameters, we relaxed the thresholds used for geometric verification, image resection (registration), triangulation and bundle rejection. This choice was made considering that PO is not static, implying that the expected number of inliers is significantly lower than in regular SfM applications. Similarly, higher image residuals may need to be accepted in the orientation, triangulation, and bundle adjustment stages. This meant increasing the reprojection error from 4 px in steps up to 50 px in the most challenging datasets B1 and B2.

Photogrammetric processing was performed on a workstation with the following characteristics:

- CPU: Intel Core i7-14700K (20 cores, 3.4 GHz)
- RAM: 32 GB DDR5 (6000 MHz)
- GPU: NVIDIA RTX 4000 Series (VRAM: 16 GB GDDR6X)
- OS: Windows 11 Pro (64-bit)

We tested the following image orientation methods:

1. Metashape proprietary algorithm (SIFT-like) (https://www.agisoft.com/);
2. COLMAP DSP-SIFT (Dong and Soatto 2015; Schonberger and Frahm, 2016);
3. DIM SuperPoint (DeTone et al., 2018) + LightGlue (Lindenberger et al., 2023);
4. DIM Disk (Tyszkiewicz et al.,2020) + LightGlue;
5. DIM Aliked (Zhao et al., 2023) + LightGlue;
6. DIM ORB (OpenCV) + Kornia nearest neighbour matcher (Riba et al., 2020);
7. DIM SIFT (OpenCV) (Riba et al., 2020) + Kornia nearest neighbour matcher;
8. DIM KeyNetAffNetHardNet (Riba et al., 2020) + nearest neighbour matcher;
9. DIM DeDoDe (Riba et al., 2020) + Kornia nearest neighbour matcher.

3. Results

For a more concise analysis of results, along with the number of images oriented over the total for each dataset, we use the match matrix from COLMAP as a visual summary to understand weaknesses of the matching stage related to the specific imaging block. Moreover, the match matrix provides a clear view of the matched images, indicating whether there was a potential to orient additional images using more relaxed thresholds. As reported in other studies (Bellavia et al., 2022; Remondino et al., 2021; Menna et al., 2020), inner metrics from bundle adjustment, such as a lower reprojection error do not necessarily correlate with a higher accuracy in object space, especially for weak camera network where systematic effects can be completely absorbed by exterior orientation within the bundle solution (Menna et al 2020). Therefore, when available, we report the metric performances of the different methods as RMSE against the collected ground truth measurements.

3.1 Dataset A: 50m long straight transect with the BlueBoat

Method 5 (Aliked + LightGlue) was the only one able to orient all 100 images (Figure 6) at quarter linear resolution (low quality parameter in DIM).

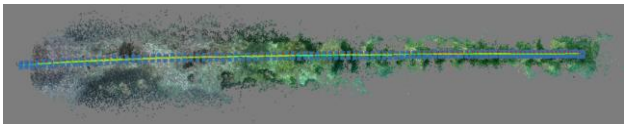

Figure 6. Straight transect as oriented by method 5 showing from left to right a reduced lateral extension of matched points as a consequence of the decreasing lateral footprint associated to the reduced depth.

All the other pipelines used could orient only the first 50 images of the dataset, observing the dead matte. At higher resolutions,

none of the methods succeeded. Analysing the match matrices at quarter image resolution, the methods 3,4,5 (section 2.4) provide a fully connected band matrix while all the other methods lack matches as the PO meadow starts to fully cover the field of view (Figure 7).

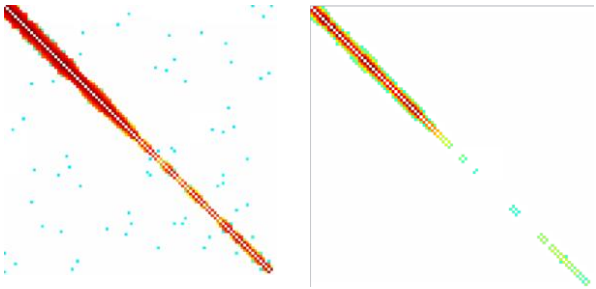

Figure 7. Example of match matrices for Method 5 (left) and Method 7 (right) showing the absence of matches between subsequent images starting from the middle of the strip where the dead matte ends and the PO meadow starts.

3.2 Dataset B1: full photogrammetric block at 15m depth - autumn

The dataset was processed at full resolution (GSD 1mm). Methods 1 (Metashape) and 3 (DIM SuperPoint + LightGlue) succeeded in orienting all the images, although Method 1 required manual interaction with the temporarily unoriented images, as described in section 2.4.
The accuracy of image orientation was visibly poor and only after adding manual image observations using the tips of the 6 poles (four at corners and two at 1/3 and 2/3 of the area with an image residuals RMS of 16 pixels), the block connectivity and consequently, image orientation, improved. Figure 8 shows the improvement achieved for Method 1 (Metashape): the lines connecting the cameras indicate that the images match between each other only as stereo cameras and along the same strip.

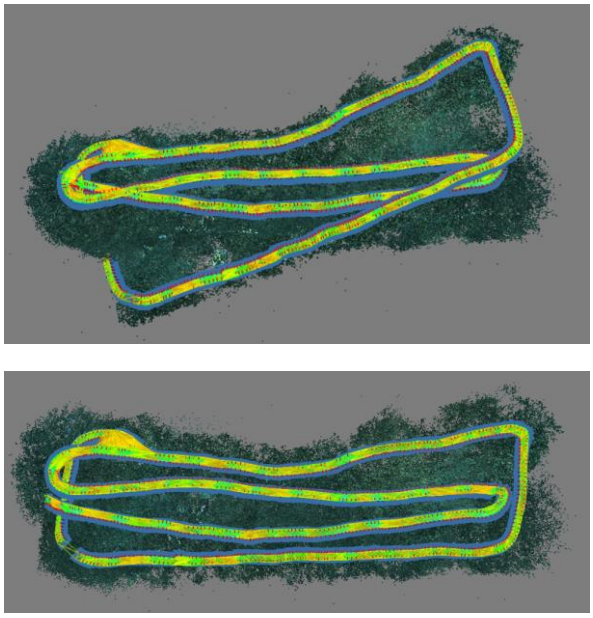

Figure 8. Dataset B1 before (up) and after (down) adding manual tie points on the six poles materialized in the PO meadow.

The only part of the imaging block where two strips are connected is at the upper left corner where the temporary calibration site was set, thus providing some artificial and more robust texture to match. Table 2 summarises the metric results for Methods 1 and 3 on dataset B1 as length measurement error (LME) against ground truth distances, $RMSE_Z$ with respect to measured poles heights and $RMSE_b$ on calibrated camera baselines.

Method	LME (7 distances)	$RMSE_Z$ (6 points)	$RMSE_b$ baselines
1.Metashape	0.47 m	0.44 m	0.02 m
3. DIM SuperPoint + LightGlue	0.44 m	0.11 m	0.008 m

Table 2. Metric performances on dataset B1.

3.3 Dataset B2: full photogrammetric block at 15m depth - winter

The original images (46MP) from Nikon D850 were processed at low quality (GSD four times larger, i.e., 1.4 mm) for time constraints, as each method, at full resolution, would last several days. Method 2 (COLMAP DSP-SIFT) was the only method that managed to orient most of the images (909/910), matching photographs belonging to adjacent and cross strips, as visible in Figure 9. Metric performances are summarised in Table 3.

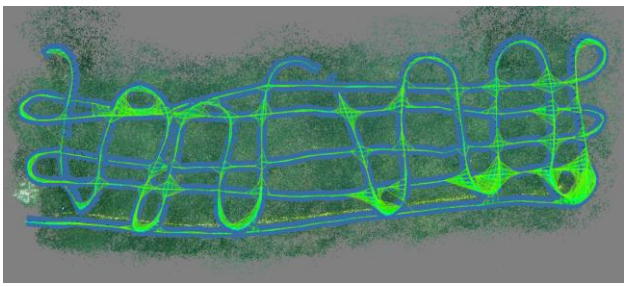

Figure 9. Graph in Metashape showing the whole imaging block with lines that connect the matching images.

	LME (7 distances)	$RMSE_Z$ (6 points)
2. COLMAP DSP-SIFT	0.03 m	0.01 m

Table 3. Metric performances on dataset B2

3.4 Dataset C: 50 square loop

As for dataset B2 we chose a quarter resolution setting (low quality, GSD 1.4mm) for time constraints. Only Method 5 (DIM Aliked + LightGlue) succeeded to match and orient the entire image sequence closing the loop (Figure 10).

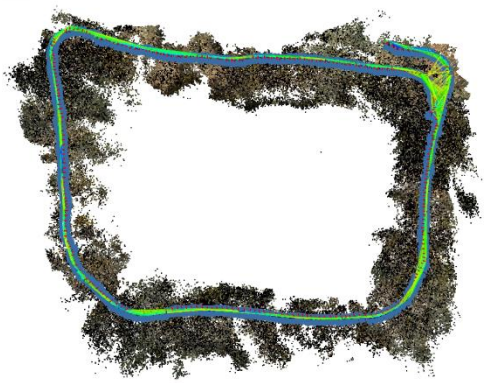

Figure 10. Loop from dataset C fully oriented only Method 5 (DIM Aliked + LightGlue).

After marking the 4 points at the end of the two scalebars (image residuals RMS of 6px) and applying the scaling on the two scalebars, the length residual was about 2 mm.

4. Discussions and conclusions

Matching the PO fully covering the field of view of the camera is a hard task, feasible only in particularly calm water conditions. Even in such conditions, it is hard to match feature points after a few seconds due to a combination of factors, as explained in section 1.4. For this reason, imaging blocks like those generally used in aerial photogrammetry with parallel and cross strips are likely to be ineffective over meadows fully covered by long PO leaves. In these cases, despite the guaranteed overlap and side lap, revisiting the same area in a cross strip or between adjacent and cross strips does not improve the "rigidity" of the imaging block. If the image acquisition is interrupted at the end of a strip to be started again at the beginning of the next adjacent strip, the tie point tracking would be interrupted, and it could be difficult to orient the images passing from one strip to another. Therefore, a continuous acquisition (for example using timelapse) is suggested even when capturing still images, taking care of joining the adjacent strips through a slower U-shaped curve trajectory. This approach fits well with vSLAM methods where feature matching and tracking are performed in real-time.

Reference points materialized as stable poles inserted in the substrate were beneficial for the overall accuracy and reliability of the survey. Therefore, they are highly recommended (see results for datasets B1 and B2) when monitoring PO meadows over time.

Continuous PO meadows might be easier to survey at the end of the winter season (dataset B2), where the less dense foliage uncovers the more stable matte substrate. In these cases, more traditional hand-crafted methods such as DSP SIFT seem to better perform for their better rotation invariance (Bellavia et al., 2022) that make them able to match across adjacent and cross strips. Among the learning-based methods, DIM Aliked + LightGlue seemed to show better performance, confirming what was also found underwater in Zhong et al (2024).

As shown in this study, there is not a winning method among those tested. The possibility to adjust the inlier and reprojection error thresholds at the different stages of SfM from matching to bundle adjustment proved beneficial giving the possibility to orient dataset B2 in COLMAP.

Further tests are currently being done for refining the outcomes presented.

Acknowledgements

This research was supported by POSEIDON - multitemPOral SEagrass mapping and monitoring of posIDONia meadows and banquettes for blue carbon conservation (E53D23021870001), a research project of Italian national relevance initiative "Italia Domani - Piano Nazionale di Ripresa e Resilienza" (PNRR) funded by the European Commission - Next Generation EU. EN and GC declares financial support was received from the National Biodiversity Future Center funded by the Italian Ministry of University and Research, PNRR, Missione 4, Componente 2, "Dalla ricerca all'impresa", Investimento 1.4 Project CN00000033.

5. References

Abadie, A., Boissery, P. and Viala, C., 2018. Georeferenced underwater photogrammetry to map marine habitats and submerged artificial structures. The Photogrammetric Record, 33(164), pp.448-469.

Appolloni, L., Buonocore, E., Russo, G.F. and Franzese, P.P., 2020. The use of remote sensing for monitoring Posidonia oceanica and Marine Protected Areas: A systemic review. Ecological Questions, 31(2), pp.7-17.

Baiocchi, V., Cianfanelli, F. and Nocerino, E., 2024. Satellite images and bathymetric LiDAR for mapping seagrass meadows: an overview. *TRENDS IN EARTH OBSERVATION*, pp.87-92.

Bellavia, F., Morelli, L., Menna, F. and Remondino, F., 2022. Image orientation with a hybrid pipeline robust to rotations and wide-baselines. *The International Archives of the Photogrammetry, Remote Sensing and Spatial Information Sciences*, 46, pp.73-80.

Bonin-Font, F., Campos, M.M. and Codina, G.O., 2016. Towards visual detection, mapping and quantification of Posidonia oceanica using a lightweight AUV. *IFAC-PapersOnLine*, 49(23), pp.500-505.

Ceccherelli, G., Chiabrando, F., Gallitto, F., Lingua, A., Longhi, V., Maschio, P., Matrone, F., Menna, F., Nocerino, E., Scalici, M. and Secco, S., 2024. Multitemporal Seagrass Mapping and Monitoring of Posidonia Meadows and Banquettes for Blue Carbon Conservation: The Poseidon Project. *The International Archives of the Photogrammetry, Remote Sensing and Spatial Information Sciences*, *48*, pp.65-71.

Chen, L., Rottensteiner, F. and Heipke, C., 2020. Deep learning based feature matching and its application in image orientation. *ISPRS Annals of the Photogrammetry, Remote Sensing and Spatial Information Sciences*, 2, pp.25-33.

Cozza, R., Rende, F., Ferrari, M., Bruno, L., Pacenza, M., Dattola, L. and Bitonti, M.B., 2019. Biomonitoring of Posidonia oceanica beds by a multiscale approach. *Aquatic Botany*, 156, pp.14-24.

Dattola, L., Rende, S.F., Dominici, R., Lanera, P., Di Mento, R., Scalise, S., Cappa, P., Oranges, T. and Aramini, G., 2018, October. Comparison of Sentinel-2 and Landsat-8 OLI satellite images vs. high spatial resolution images (MIVIS and WorldView-2) for mapping Posidonia oceanica meadows. In *Remote Sensing of the Ocean, Sea Ice, Coastal Waters, and Large Water Regions* 2018 (Vol. 10784, pp. 252-262). SPIE.

DeTone, D., Malisiewicz, T. and Rabinovich, A., 2018. SuperPoint: Self-supervised interest point detection and description. In *Proceedings of the IEEE conference on computer vision and pattern recognition workshops* (pp. 224-236).

Dong, J. and Soatto, S., 2015. Domain-size pooling in local descriptors: DSP-SIFT. In *Proceedings of the IEEE conference on computer vision and pattern recognition* (pp. 5097-5106).

Lindenberger, P., Sarlin, P.E. and Pollefeys, M., 2023. LightGlue: Local feature matching at light speed. In *Proceedings of the IEEE/CVF International Conference on Computer Vision* (pp. 17627-17638).

Mandlburger, G., 2022. A review of active and passive optical methods in hydrography. *The International Hydrographic Review*, (28), pp.8-52.

Marre, G., Deter, J., Holon, F., Boissery, P. and Luque, S., 2020. Fine-scale automatic mapping of living Posidonia oceanica seagrass beds with underwater photogrammetry. *Marine Ecology Progress Series*, 643, pp.63-74.

Menna, F., Nocerino, E. and Calantropio, A., 2024. High-accuracy height differences using a pressure sensor for ground control points measurement in underwater photogrammetry. T*he International Archives of the Photogrammetry, Remote Sensing and Spatial Information Sciences*, 48, pp.273-279.

Menna, F., Nocerino, E., Ural, S. and Gruen, A., 2020. Mitigating image residuals systematic patterns in underwater photogrammetry. *The International Archives of the Photogrammetry, Remote Sensing and Spatial Information Sciences, 43*, pp.977-984.

Menna, F., Nocerino, E., Drap, P., Remondino, F., Murtiyoso, A., Grussenmeyer, P. and Börlin, N., 2018. Improving underwater accuracy by empirical weighting of image observations. *The International Archives of the Photogrammetry, Remote Sensing and Spatial Information Sciences, 42*, pp.699-705.

Menna, F., Nocerino, E., Fassi, F. and Remondino, F., 2016. Geometric and optic characterization of a hemispherical dome port for underwater photogrammetry. *Sensors*, 16(1), p.48.

Morelli, L., Ioli, F., Maiwald, F., Mazzacca, G., Menna, F. and Remondino, F., 2024. Deep-image-matching: a toolbox for multiview image matching of complex scenarios. *The International Archives of the Photogrammetry, Remote Sensing and Spatial Information Sciences*, *48*, pp.309-316.

Nocerino, E., Menna, F. and Verhoeven, G.J., 2022. Good vibrations? How image stabilisation influences photogrammetry. *The International Archives of the Photogrammetry, Remote Sensing and Spatial Information Sciences*, *46*, pp.395-400.

Pansini, A., Berlino, M., Mangano, M.C., Sarà, G. and Ceccherelli, G., 2025. Meta-analysis reveals the effectiveness and best practices for the iconic Mediterranean seagrass restoration. *Science of the Total Environment*, *976*, p.179325.

Remondino, F., Menna, F. and Morelli, L., 2021. Evaluating hand-crafted and learning-based features for photogrammetric applications. *The International Archives of the Photogrammetry, Remote Sensing and Spatial Information Sciences*, *43*, pp.549-556.

Rende, S.F., Bosman, A., Menna, F., Lagudi, A., Bruno, F., Severino, U., Montefalcone, M., Irving, A.D., Raimondi, V., Calvo, S. and Pergent, G., 2022. Assessing seagrass restoration actions through a micro-bathymetry survey approach (Italy, mediterranean sea). *Water*, *14(8)*, p.1285.

Rende, S.F., Bosman, A., Di Mento, R., Bruno, F., Lagudi, A., Irving, A.D., Dattola, L., Giambattista, L.D., Lanera, P., Proietti, R. and Parlagreco, L., 2020. Ultra-high-resolution mapping of Posidonia oceanica (L.) delile meadows through acoustic, optical data and object-based image classification. *Journal of Marine Science and Engineering*, *8*(9), p.647.

Rende, F.S., Irving, A.D., Lagudi, A., Bruno, F., Scalise, S., Cappa, P., Montefalcone, M., Bacci, T., Penna, M., Trabucco, B. and Di Mento, R., 2015. Pilot application of 3D underwater imaging techniques for mapping Posidonia oceanica (L.) Delile meadows. *The International Archives of the Photogrammetry, Remote Sensing and Spatial Information Sciences*, *40*, pp.177-181.

Riba, E., Mishkin, D., Ponsa, D., Rublee, E. and Bradski, G., 2020. Kornia: an open source differentiable computer vision library for pytorch. In *Proceedings of the IEEE/CVF Winter Conference on Applications of Computer Vision* (pp. 3674-3683).

Russo, F., Del Pizzo, S., Di Ciaccio, F. and Troisi, S., 2023. An enhanced photogrammetric approach for the underwater surveying of the Posidonia meadow structure in the Spiaggia Nera area of Maratea. *Journal of Imaging*, 9(6), p.113.

Schonberger, J.L., Hardmeier, H., Sattler, T. and Pollefeys, M., 2017. Comparative evaluation of hand-crafted and learned local features. In Proceedings of the IEEE conference on computer vision and pattern recognition (pp. 1482-1491).

Schonberger, J.L. and Frahm, J.M., 2016. Structure-from-motion revisited. In *Proceedings of the IEEE conference on computer vision and pattern recognition* (pp. 4104-4113).

Vassallo, P., Paoli, C., Rovere, A., Montefalcone, M., Morri, C. and Bianchi, C.N., 2013. The value of the seagrass Posidonia oceanica: A natural capital assessment. *Marine pollution bulletin*, *75*(1-2), pp.157-167.

Zhao, X., Wu, X., Chen, W., Chen, P.C., Xu, Q. and Li, Z., 2023. Aliked: A lighter keypoint and descriptor extraction network via deformable transformation. *IEEE Transactions on Instrumentation and Measurement*, *72*, pp.1-16.

Zhong, J., Li, M., Gruen, A., Gong, J., Li, D., Li, M. and Qin, J., 2024. Application of Photogrammetric Computer Vision and Deep Learning in High-Resolution Underwater Mapping: A Case Study of Shallow-Water Coral Reefs. *ISPRS Annals of the Photogrammetry, Remote Sensing and Spatial Information Sciences*, *10*, pp.247-254.